Available online at www.eccomasproceedia.org
Eccomas Proceedia SMART (2023) 1491-1496

ECCOMAS
Proceedia

X ECCOMAS Thematic Conference on Smart Structures and Materials
SMART 2023
D.A. Saravanos, A. Benjeddou, N. Chrysochoidis and T. Theodosiou (Eds)

SURFACE ROUGHNESS CHARACTERIZATION OF NITINOL SAMPLES FABRICATED USING LASER POWDER BED FUSION

WAEL ZAKI*, ADRIANO CIBRIAN CARCAVILLA*

* Advanced Digital and Additive Manufacturing center
Khalifa University of Science and Technology
P.O. Box 127788, Abu Dhabi
United Arab Emirates
email: wael.zaki@ku.ac.ae, www.ku.ac.ae

Abstract. The determination of optimal process parameters for additively manufactured nitinol typically requires the characterization of a large batch of test samples. Such characterization, which involves microstructural and structural analysis, is resource intensive. In this work, we propose the use of bulk surface roughness characterization by means of instrumented optical profilometry to identify, among many nitinol samples fabricated using laser powder bed fusion, a group that is likely to possess good structural integrity. The approach assumes that samples of high relative density are unlikely to display mediocre surface quality. The samples considered for the analysis are fabricated using laser powder bed fusion considering variations in laser power and scanning speed. The rest of the parameters were selected based on reported literature with the aim of producing predominantly dense samples. Plots of surface roughness data against each laser power, scanning speed, and input energy density show three distinct regions characterized by noticeably different slopes. The region with the lowest slope is found to be associated with samples having the lowest roughness. The flat portions of the curves span a relatively wide range of process parameters, indicating that samples with minimal surface roughness are obtainable for many combinations of process parameters. The findings of this work may help guide the choice of laser powder bed fusion parameters that would produce quality as-fabricated nitinol samples.
.

Key words: Nitinol, Shape Memory Alloys, Additive Manufacturing, Laser Powder Bed Fusion, Surface Roughness, Process Parameters.

1 INTRODUCTION

The functional behavior of shape memory alloys (SMAs) has long attracted interest toward its many potential engineering applications. To date, nitinol remains the most researched SMA, due to its many interesting structural and functional properties, including elevated yield strength, high strain recovery, good fatigue resistance, low toxicity, and high biocompatibility and corrosion resistance. Despite these appealing characteristics, the integration of nitinol in

Peer-review under responsibility of the organizing committee of SMART 2023.
doi: 10.7712/150123.9920.444283

engineering solutions is challenging because of several well-documented reasons, including poor workability and elevated hardness and tool ware. These shortcomings are naturally alleviated when nitinol is fabricated using additive manufacturing (AM) methods [1]–[3]. Indeed, additive manufacturing allows direct fabrication of parts of seemingly arbitrary complexity directly from computer-aided design (CAD), without requiring the use of tools and with typically minimal waste of material feedstock. Additive manufacturing, which englobes a wide variety of fabrication methods, refers to a fabrication process by which structures are fabricated by the deposition and joining of successive material layers according to patterns corresponding to cross-sections of three-dimensional CAD models [4], [5]. Depending on the state of the feedstock and its deposition and joining methods, additive manufacturing processes are classified into the following seven categories: sintering, binding, melting, lamination, extrusion, and polymerization. The first three are applicable to solid material in powder state, whereas the fourth is applicable to non-powdered solids, and the last two to feedstock in liquid state. Several AM processes have been successfully utilized in fabricating nitinol samples, including laser- and electron-beam powder bed fusion [1], and extrusion of nitinol-enriched polymer filaments [6] resulting in so-called *green* nitinol parts that are then sintered. The present work focuses on laser powder bed fusion of monolithic nitinol samples using laser powder bed fusion (LPBF) using many combinations of process parameters. Characterization of the surface roughness of the samples shows non-monotonic variation in terms of laser power, scanning speed and input energy density. The results may be used to carry out rapid initial elimination of sub-optimal combinations of process parameters, thereby facilitating subsequent optimization of process parameters by restricting their design space.

In addition to this introduction, the paper is organized into a materials and methods section, which introduces the nitinol feedstock powder used and details of the experimental and data analysis procedures; a results and discussions section, which presents and analyzes data and figures representing the main findings; and a final section dedicated to conclusions and outlook.

2 MATERIALS AND METHODS

Nickel-rich nitinol powder of particle size between 15 and 53 μm was procured from TLS Technik GmbH & Co. Spezialpulver KG. The chemical composition of the powder consists of 55.6 wt.% Ni, 0.008 wt.% C, 0.04 wt.% O, 0.002 wt.% N, 0.02 wt.% Fe, 0.0008 wt.% H, and a balance of Ti. The nitinol powder was used to fabricate dense nitinol samples, of cylindrical shape, on an EOS M400-4 metal 3D printer. The fabricated samples, 6 mm in height and 5 mm in diameter, are obtained using laser power between 40 and 250 W. For each laser power value, scanning speeds are selected to achieve an energy input density between 83 and 125 J/m^3. These limit values of the energy density are selected, based on extensive literature review, for successful printing of dense nitinol. Intermediate, near-evenly spaced energy densities are also considered, for a total of 11 different values corresponding to as many different values of scanning velocity. The combinations of laser power and scanning speeds correspond to a total of 232 different sets of process parameters, each of which used to print one cylindrical test sample. The samples were printed on two 10 cm × 10 cm build plates. Roughness measurements were carried out on the top surface of each sample using an Alicona Infinite Focus optical profilometer without having to separate the samples from their base plates. The

profilometer allows non-contact characterization of surface roughness. For simplicity, roughness measurements, for each sample, are carried out over a rectangular subdomain of the surface being observed. The data is processed to determine an average roughness of the observed square domain, which is considered here to be representative of that of the entire free surface. Processing of the data involved filtering out low-frequency warping and surface deformations caused by imperfections of the recoater blade as well as thermal warping. The arithmetic average R_a of a subset of the sampled surface roughness data is shown in Figure 1.

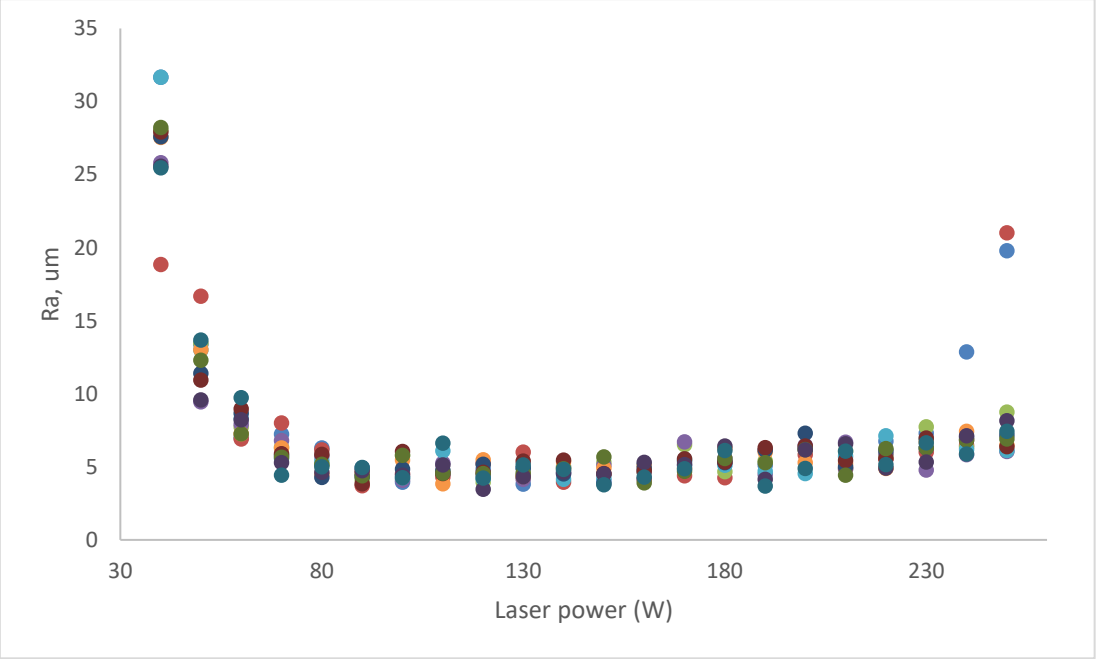

Figure 1. Average surface roughness for laser power values between 40 W and 250 W. For each laser power, 11 different values of scanning speed are reported, corresponding to 11 input energy densities.

Each data point on the figure represents the average roughness of a single sample obtained with a laser power in the range 40 to 250 W and one of 11 different combinations of scanning speeds, resulting in as many different values of input energy density. The figure reveals a steep decrease in surface roughness, from 32 μm to approximately 5 μm, as the laser power is decreased from 40 to 80 W. The decrease is observed irrespective of scanning speeds. Between 30 and around 200 W of laser power, roughness seems to stabilize before increasing again. For the two highest laser power values, data points represented in blue and red colors are seen to substantially deviate from the general trend. Such deviation is indicative of amplified influence on roughness of the scanning speeds used to fabricate the corresponding samples.

For the same samples, the influence of input energy density on roughness is illustrated in Figure 2.

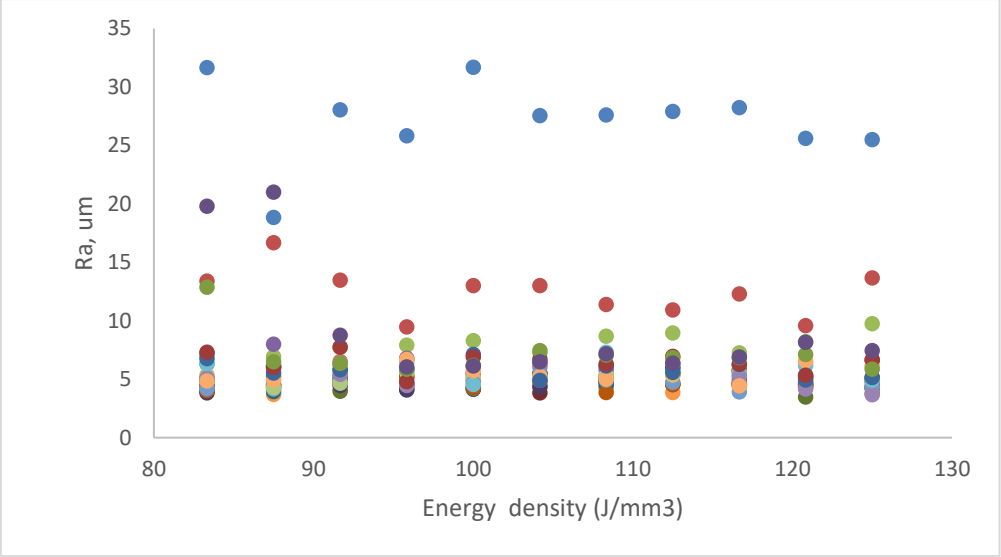

Figure 2. Average surface roughness for input energy density between 83 J/mm^3 and 125 J/mm3. The different colors represent 11 different values of laser power.

Roughness does appear to initially drop with increasing energy density for the data sets shown in blue, red, and violet, which correspond to the lowest considered values of laser power. The observed trend is explained by improved melting of the powder with increased energy input. Moreover, the figure shows that input energy does not fully determine roughness, as confirmed by the clear vertical spread in data points associated with the same energy density.

The influence of scanning speed on roughness is plotted in Figure 3.

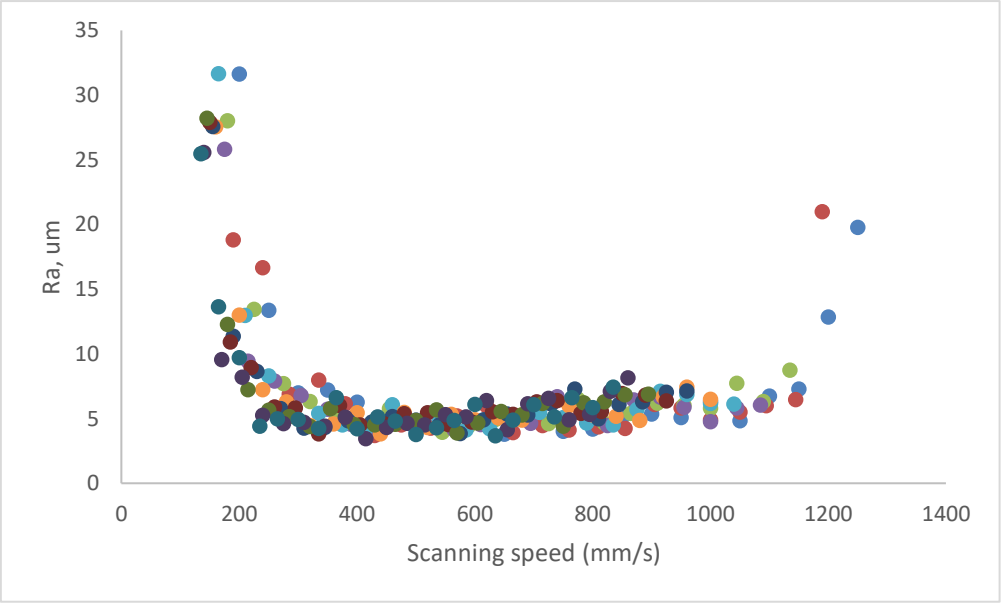

Figure 3. Average surface roughness for scanning speeds between 135 mm/s and 1250 mm/s. The different colors represent 11 different values of laser power.

The plotted data shows increased roughness toward the outer boundaries of the considered range of scanning speeds, with minimal and mostly constant roughness values toward the middle. This is explained by higher scanning speed resulting in poor powder fusion, whereas lower speeds excessively disturb the fusion bed resulting in increased roughness as the melt solidifies.

3 CONCLUSIONS AND OUTLOOK

Optical profilometry was used in this work to rapidly investigate the surface roughness of a large number of nitinol samples fabricated using laser powder fusion. The obtained data was plotted in terms of laser power, scanning speed, and input energy density, keeping the rest of the process parameters fixed. Examination of the plotted data led to the following conclusions:

- For the range of parameters considered and across all input energy values, roughness initially decreases with increasing laser power then stabilizes. Surface roughness is mostly indistinguishable for samples on the flat sections of the curves.
- Examination of surface roughness evolution in terms of energy input density shows that the latter is not uniquely correlated to roughness. Laser power plays an important role at identical levels of energy input.
- The change in surface roughness with scanning speed, all other process parameters being identical, shows minimal roughness at intermediate speeds. This is explained by higher speeds resulting in insufficient melting, whereas lower speeds may be causing increased disturbance of the fusion bed, leading to roughness as the bed solidifies.

The results reported here did not consider the full set of samples fabricated over the considered space of process parameters. Closer investigation of the data will be carried out in future work for cases where data points are not clearly distinguishable, with possible consideration of a large set of samples.

ACKNOWLEDGEMENT

The corresponding author would like to acknowledge the financial support of Khalifa University through internal research grant CIRA 2021-099.

REFERENCES

[1] A. N. Alagha, S. Hussain, and W. Zaki, “Additive manufacturing of shape memory alloys: A review with emphasis on powder bed systems,” *Materials and Design*, vol. 204. Elsevier Ltd, p. 109654, Jun. 2021. doi: 10.1016/j.matdes.2021.109654.

[2] M. Elahinia, N. Shayesteh Moghaddam, M. Taheri Andani, A. Amerinatanzi, B. A. Bimber, and R. F. Hamilton, “Fabrication of NiTi through additive manufacturing: A review,” *Progress in Materials Science*. 2016. doi: 10.1016/j.pmatsci.2016.08.001.

[3] A. C. Carcavilla and W. Zaki, “Fatigue of Shape Memory Alloys With Emphasis on Additively Manufactured NiTi Components,” *Appl Mech Rev*, vol. 74, no. 4, Jul. 2022, doi: 10.1115/1.4055175.

[4] N. V. Viet, N. Karathanasopoulos, and W. Zaki, “Mechanical attributes and wave propagation characteristics of TPMS lattice structures,” *Mechanics of Materials*, vol. 172, Sep. 2022, doi: 10.1016/j.mechmat.2022.104363.

[5] A. N. Alagha, V. Nguyen, and W. Zaki, “Effective phase transformation behavior of NiTi triply periodic minimal surface architectures,” *https://doi.org/10.1177/1045389X221115704*, Aug. 2022, doi: 10.1177/1045389X221115704.

[6] M. A. Wagner, J. L. Ocana-Pujol, A. Hadian, F. Clemens, and R. Spolenak, “Filament extrusion-based additive manufacturing of NiTi shape memory alloys,” *Mater Des*, vol. 225, Jan. 2023, doi: 10.1016/j.matdes.2022.111418.